Journal of Pain Research

Dovepress
Taylor & Francis Group

Open Access Full Text Article

ORIGINAL RESEARCH

Identifying Diagnostic Biomarkers for Electroacupuncture Treatment of Rheumatoid Arthritis Using Bioinformatic Analysis and Machine Learning Algorithms

Yijun Sun, Guoqi Dong, Hui Gao, Yong Yao, Huayuan Yang

School of Acupuncture-Moxibustion and Tuina, Shanghai University of Traditional Chinese Medicine, Shanghai, 201203, People's Republic of China

Correspondence: Huayuan Yang, School of Acupuncture-Moxibustion and Tuina, Shanghai University of Traditional Chinese Medicine, Shanghai, 201203, People's Republic of China, Email yhy4@shutcm.edu.cn

Purpose: Rheumatoid arthritis (RA) is a persistent inflammatory condition, and electroacupuncture (EA) has been demonstrated to effectively reduce the symptoms associated with RA. However, the molecular mechanisms underlying the effects of EA in RA remained poorly understood. This study aimed to identify potential diagnostic biomarkers for RA and elucidated the molecular targets of EA by using bioinformatics analysis and machine learning algorithms in peripheral blood samples.

Methods: We obtained datasets from the Gene Expression Omnibus(GEO) database containing samples from RA patients (GSE15573) and from RA patients after EA treatment (GSE59526) for bioinformatics analysis. Diagnostic biomarkers were identified using three distinct machine learning algorithms (LASSO, Random Forest and SVM-REF). A rat model of RA was established using Complete Freund's Adjuvant (CFA), and quantitative real-time PCR was performed to confirm the differential expression of identified diagnostic biomarkers and assess the modulatory impact of EA on these genes.

Results: Twenty-six genes were identified as differentially expressed following EA treatment. Three machine learning algorithms converged on ARHGAP17 and VEGFB as potential diagnostic biomarkers for RA, exhibiting robust diagnostic performance (AUC > 0.75) and consistent expression patterns across multiple RA cohorts (GSE17755, GSE205962 and GSE93272). Besides, EA treatment significantly increased the paw withdrawal threshold (PWT) and the peripheral blood expression of both ARHGAP17 and VEGFB in CFA rats.

Conclusion: This study employed three machine learning algorithms to identify potential diagnostic biomarkers for the alleviation of RA by EA. The biomarkers demonstrated robust diagnostic performance across multiple validation datasets. Furthermore, animal experiments confirmed that EA exerted a favorable regulatory effect on these diagnostic biomarkers. The findings of this study provided novel therapeutic targets for the EA treatment of RA.

Keywords: rheumatoid arthritis, machine learning, bioinformatics, diagnostic biomarkers, electroacupuncture

Introduction

Rheumatoid arthritis (RA) is the most prevalent chronic inflammatory arthritis, which can cause progressive destruction of joint cartilage.[1] RA can manifest at any age, with its peak incidence typically observed in individuals aged 30–60. As a challenging chronic condition, RA significantly impairs patients' quality of life and imposes substantial societal and economic burdens. With a prevalence of approximately 0.3% to 1%, RA is often associated with various chronic diseases, further exacerbating healthcare demands and caregiving responsibilities.[2]

Currently, radical treatment for RA is limited. The therapeutic management of RA predominantly involves non-steroidal anti-inflammatory drugs (NSAIDs), conventional biological disease-modifying antirheumatic drugs (DMARDs), glucocorticoids, and other pharmacological interventions. These approaches aim to mitigate inflammation, retard disease progression, and optimize patients' quality of life.[3] However, the side effects of these drugs are controversial. Acupuncture has been practiced in Asia for over two millennia as a complementary and alternative therapeutic modality.[4] Clinical studies have

Received: 5 February 2025
Accepted: 25 June 2025
Published: 5 July 2025

shown that electroacupuncture (EA) significantly relieved pain and joint swelling in RA patients and improved their quality of life without significant adverse effects.[5–7] Preclinical studies have also shown that EA can significantly improve the levels of pro-inflammatory factors in the peripheral blood of RA patients to improve the internal environment for the development and progression of RA.[8,9] Identifying the targeted genes underlying the therapeutic effects of EA in alleviating RA can provide critical insights for further mechanistic investigations[10] and facilitate the development of standardized treatment protocols.[11] However, the exact target genes of EA for RA, especially in peripheral blood, remained unidentified.

With the development of gene microarray and bioinformatics technologies, more and more studies were focused on exploring the mechanisms of RA occurrence and key genes at the transcriptomic level.[12,13] In the context of precision medicine and personalized health care, Traditional Chinese Medicine (TCM) has received increasing attention for providing personalized medical services based on TCM theories. Several studies have utilized bioinformatics analysis to identify hub targets involved in the pathogenesis of RA and validated the regulatory effects of Chinese herbal medicine on these hub targets through animal experiments. Furthermore, network pharmacology approaches were employed to elucidate the bioactive components responsible for the therapeutic efficacy.[14,15] These findings provided valuable references for identifying key targets underlying EA-mediated RA alleviation. Current studies primarily aimed to elucidate how EA alleviates RA by modulating phenotype-specific genes,[16,17] yet there remained a paucity of research employing bioinformatics technologies to systematically identify EA-targeted genes for RA treatment. Given the limited availability of gene targets for EA in RA, this study aimed to fill this gap by identifying the diagnostic markers for EA treatment in RA using bioinformatics tools and machine learning algorithms.

This research retrieved mRNA expression datasets related to RA from the GEO database. The differentially expressed genes (DEGs) of RA in peripheral blood compared to normal samples and the DEGs altered by EA were obtained by differential analysis, respectively, and 26 DEGs associated with EA for RA were obtained by taking the intersection. Two diagnostic-related genes were identified by three machine learning methods, and the diagnostic efficacy of the two genes was evaluated by constructing diagnostic models. Furthermore, we determined the regulatory effects of EA on two diagnostic-related genes using qPCR.

Materials and Methods

Dataset Collection

The RA relative microarray datasets were downloaded from the Gene Expression Omnibus (GEO) database (https://www.ncbi.nlm.nih.gov/geo/ and Table 1). Transcriptome data for GSE15573 and GSE59526 were obtained from peripheral blood. GSE15573 contained 15 normal samples and 18 RA samples, and GSE59526 contained 8 RA samples and 7 samples treated with EA. Transcriptome data for GSE17755, GSE205962, and GSE93272 were obtained from peripheral blood. GSE17755 contained 53 normal samples with 112 RA samples and GSE205962 contained 4 normal samples with 16 RA samples. To compare differences in the regulation of RA peripheral blood target genes by EA and drugs, blood samples associated with disease-modifying antirheumatic drugs (DMARDs) were downloaded from a dataset (GSE93272) containing 43 normal samples, 115 RA samples, 40 samples treated with infliximab (IFX), 37 samples treated with methotrexate (MTX), and 40 samples treated with tocilizumab (TCZ). The GSE15573 dataset was normalized using the "normalize quantiles" function in BeadStudio Software. The GSE59526 and GSE93272 datasets were normalized using the MAS 5.0 algorithm in GeneSpring

Table 1 The Details of Gene Expression Datasets

Dataset	Platform	Tissue	Normal	RA-patients	EA	IFX	MTX	TCZ
GSE15573	GPL6102	Peripheral Blood	15	18	0	0	0	0
GSE59526	GPL570	Peripheral Blood	0	8	7	0	0	0
GSE17755	GPL1291	Peripheral Blood	53	112	0	0	0	0
GSE205962	GPL16043	Peripheral Blood	4	16	0	0	0	0
GSE93272	GPL570	Peripheral Blood	43	115	0	40	37	40

Software. The GSE17755 dataset was normalized by global ratio median normalization. The GSE205962 dataset was analyzed using the RMA method with Affymetrix default analysis settings, applying global scaling as the normalization method. According to item 1 and 2 of Article 32 of the Measures for Ethical Review of Life Science and Medical Research Involving Human Subjects (dated February 18, 2023, China), this part of the bioinformatics analysis in this study was exempt from ethical approval.

Identification of Differentially Expressed Genes (DEGs) Related to EA in RA

The filtering threshold was as follows: P-value < 0.05 and |log2-fold change| ≥ 0.1. DEGs related to RA were identified by comparing normal people with RA patients. DEGs related to EA treatment were identified by comparing RA patients with those who received EA treatment. By taking the intersection of DEGs related to RA and DEGs related to EA treatment, we obtained DEGs related to EA in RA.

Identification of Diagnostic Biomarkers for RA Patients

Diagnostic biomarkers were identified using three distinct machine learning algorithms. Specifically, the least absolute shrinkage and selection operator (LASSO) algorithm was implemented using the "glmnet" package to identify potential biomarkers, with parameters set at alpha = 1, nlambda = 100, and λmin determined as the optimal λ. LASSO effectively reduces subset size and serves as a biased estimator for handling complex collinearity. It is also efficient in selecting a limited set of predictive features. The advantages of the random forest algorithm include minimal tuning of hyperparameters and handling non-linear relationships. It also has the capability to predict continuous variables with a high degree of accuracy, sensitivity, and specificity,[18] as demonstrated in this study using the "randomForest" package with nTree = 500 as the specified parameters. The top ten genes exhibiting mean decrease Gini (MDG) were identified as potential biomarkers. The support vector machine recursive feature elimination (SVM-RFE) technique is utilized to prevent overfitting and is a commonly used discriminant method for regression, classification, and pattern recognition analyses. It can improve the discriminative ability of biomarkers in classification and regression tasks, while effectively removing irrelevant features. This method was implemented using the "e1071" package, and the performance was evaluated based on the average misjudgment rates obtained from 10-fold cross-validations. The strategic integration of these three machine learning algorithms enhanced the confidence in selected biomarkers through complementary feature selection paradigms.

Establishment and Evaluation of Nomogram

The Nomogram model was developed using the "rms" package to generate calibration curves and clinical decision curves, facilitating the evaluation of clinical utility and discriminative performance of the model in the context of RA. Additionally, the "pROC" package was utilized to compute the area under the receiver operating characteristic (ROC) curve along with 95% confidence intervals (CI).

Animals

Eighteen specific pathogen free (SPF) male Sprague-Dawley (SD) rats aged 8 weeks weighing 160–200 g were procured from Shanghai B&K Laboratory Animals Co., Ltd. and accommodated in the Experimental Animal Center of Shanghai University of Traditional Chinese Medicine. The rats were provided with free access to food and water within a 12-hour light-dark cycle. All animal handling protocols adhered to the guidelines set forth by the National Research Council's Guide for the Care and Use of Laboratory Animals and were sanctioned by the Experimental Animal Ethics Committee of Shanghai University of Traditional Chinese Medicine (PZSHUTCM2401080014).

Model Establishment

Eighteen rats were divided into three groups using random assignment (n = 6 per group): (1) Control group, (2) CFA group and (3) CFA + EA group. In the CFA and CFA + EA groups, the CFA model was prepared according to previous research. Rats were anesthetized with 2–3% isoflurane (RWD Life Science Company, Shenzhen, Guangdong, China) and

100 μL CFA suspension was injected into the right hindpaw of the rats, while saline was administered to the control group.[19] Successful model induction was evidenced by the development of ipsilateral paw edema and mechanical allodynia in rats post-modeling.

Evaluation of Pain-Response Behavior

The paw withdrawal threshold (PWT) was assessed using an electronic von Frey anesthesiometer (IITC 2391, USA) following the methodology described by Vivancos.[20] This test was conducted to observe the progression of mechanical allodynia in CFA-induced rats and to evaluate the analgesic efficacy of EA. Rats underwent testing on day 0 before the model was created, as well as on days 1, 3, and 7 following EA. Before each evaluation, the rats were acclimated in Plexiglas enclosures for a period of 30 minutes. The pressure was applied to the midplantar area of the hindpaw using a polypropylene tip connected to an electronic von Frey device. The threshold for response was automatically measured when the hindpaw reacted to the pressure. The mean value of three consecutive measurements of the PWT was calculated for each paw after recording it thrice with a 5-minute interval between each measurement.

EA Treatment

Stainless steel needles (0.25 × 40 mm, Huatuo) were inserted into the Kunlun (BL60) and Zusanli (ST36) acupoints on the right side to a depth of about 5 mm. A 2 Hz, 1 mA electrical signal was administered on the needles daily for 30 minutes using a stimulation device (Model G6805-2A; Shanghai Huayi Co., Shanghai, China). The treatment with EA started on the first day after the surgery and continued for 7 days. Following the final PWT assessment, the rats were anesthetized with isoflurane (5%) and blood samples were collected from the abdominal aorta into ethylenediaminetetraacetic acid (EDTA) tubes. Subsequently, the rats were euthanized via cervical dislocation, and their peripheral blood was gathered for further biological investigations.

Real-Time Fluorescence Quantitative PCR

The results of our bioinformatics analysis were confirmed by qPCR validation of peripheral blood samples from all rats. The primers utilized have been documented in Table 2. Total RNA was isolated with a total RNA extraction solution following the manufacturer's protocol (Servicebio, Wuhan, China). Three individual reactions were conducted for every sample, with the average and standard deviation computed for each data point. The $2^{-\Delta\Delta CT}$ method was employed to quantify mRNA expression levels of diagnostic biomarkers, with GAPDH serving as the internal reference.

Statistical Analysis

The experimental data was statistically analyzed based on the GraphPad Prism software and presented as the mean ± standard deviation (SD). Statistical analysis of the control, CFA, and CFA + EA groups was performed using One-way ANOVA followed by Bonferroni post hoc tests applied for qPCR analysis, while behavioral analysis was conducted using two-way ANOVA with Bonferroni post hoc testing. A P-value of less than 0.05 was considered statistically significant for all analyses.

Table 2 Specific Primer Sequences Used in qPCR

Gene	Primer sequences (5′-3′)
ARHGAP17	F: GTGTGCAGGATCAAGACAAAAAACT
	R: CTCTCCGGGGAAGAACCAATC
VEGFB	F: GAAGAAAGTGGTGTCATGGATAGAT
	R: CTGGGCACGAGTTGTTTGAC
GAPDH	F: CTGGAGAAACCTGCCAAGTATG
	R: GGTGGAAGAATGGGAGTTGCT

Results

Screening of DEGs Related to EA in RA

The differential expression analysis revealed 2428 DEGs related to RA, with 1671 downregulated and 757 upregulated genes (Figure 1A and B). Similarly, a total of 486 DEGs related to EA treatment were identified, with 228 downregulated and 258 upregulated genes (Figure 1C and D). By taking the intersection of two groups of DEGs, a total of 26 DEGs related to EA in RA were identified (Figure 1E).

Determination of the Diagnostic Biomarkers

As shown in Figure 2A and B, the LASSO regression algorithm identified ten potential candidate biomarkers. Then, the random forest algorithm determined the top ten candidate genes ranked by MeanDecreaseGini (Figure 2C and D). As for SVM-RFE, when the number of features was 9, the accuracy was maximized (Figure 2E), and the error was minimized (Figure 2F). After combining the results of three algorithms, two diagnostic biomarkers were identified: VEGFB and ARHGAP17 (Figure 2G).

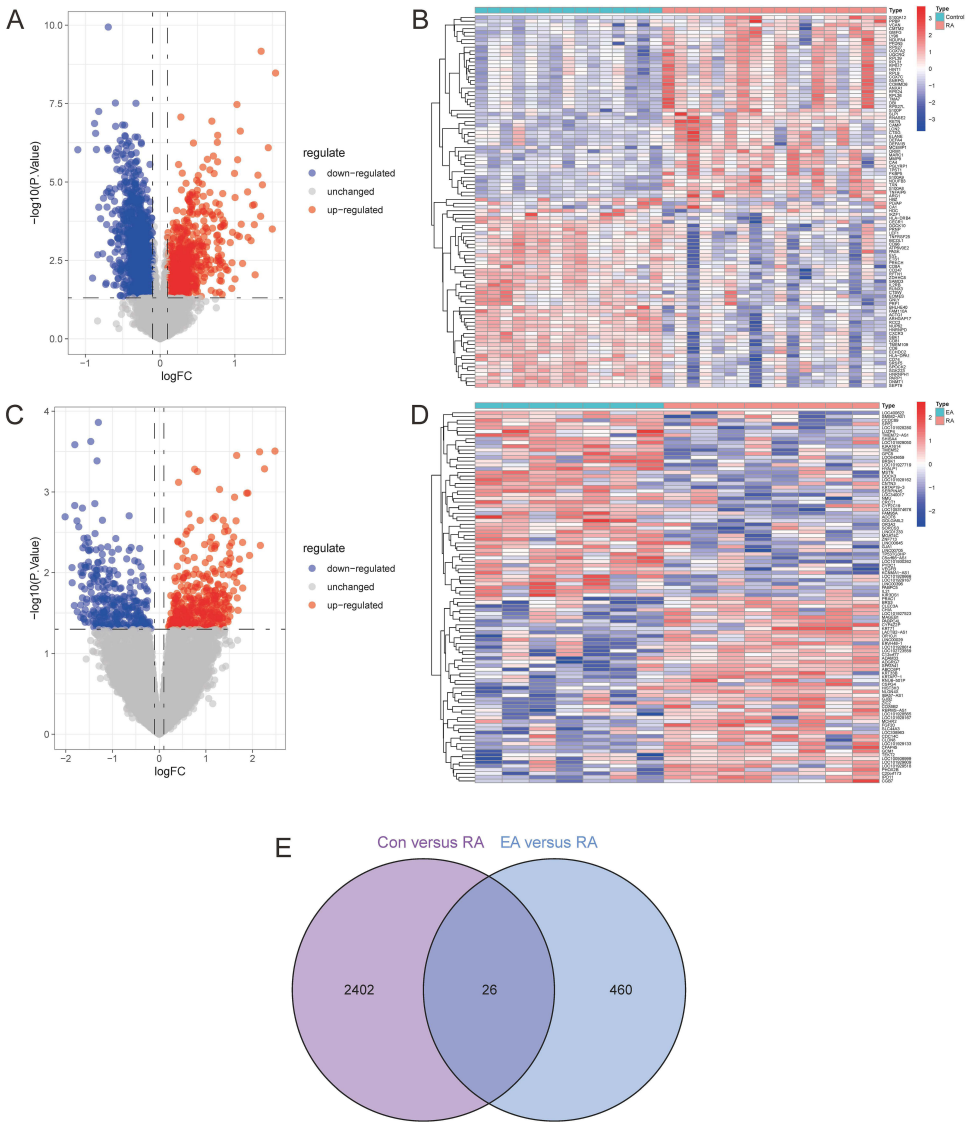

Figure 1 Identification of DEGs related to EA in RA. The volcano plot (**A**) and heatmap (**B**) for DEGs related to RA. The volcano plot (**C**) and heatmap (**D**) for DEGs related to EA treatment. (**E**) Venn diagram of the intersection of DEGs related to RA and DEGs related to EA treatment.

https://doi.org/10.2147/JPR.S517733

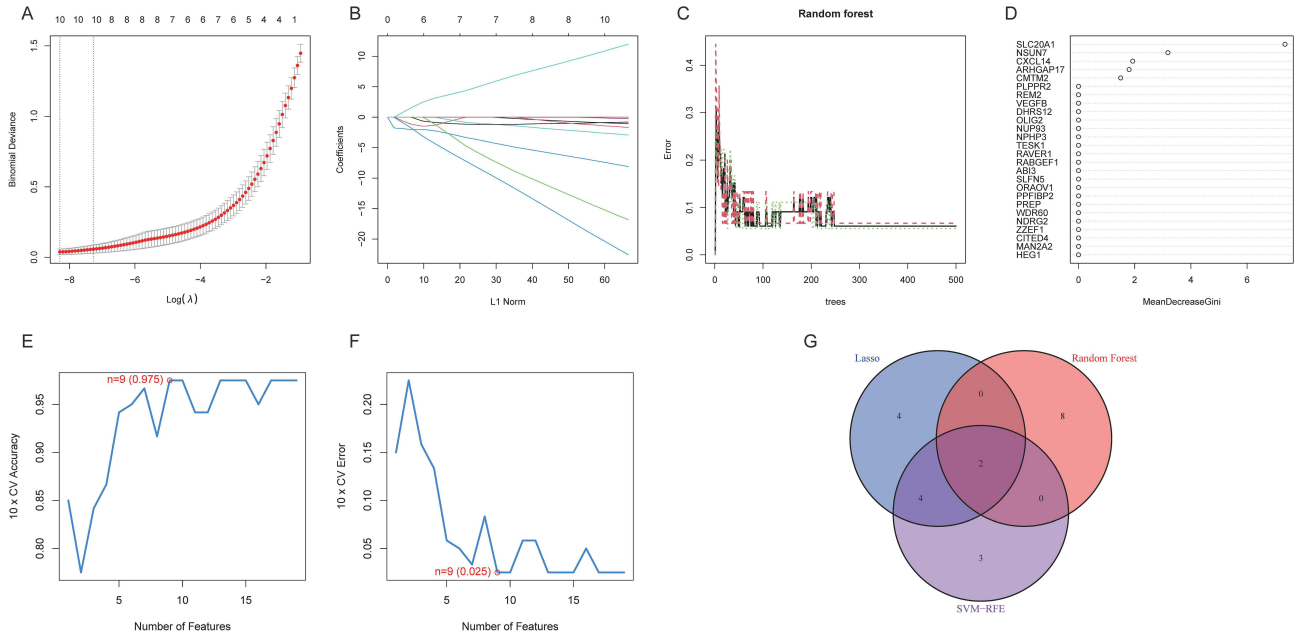

Figure 2 Identification of diagnostic biomarkers. The lambda values (**A**) and minimum (**B**) of diagnostic biomarkers were identified by LASSO. (**C**) Potential diagnostic biomarkers selection via Random Forest. (**D**) MeanDecreaseGini showed the rank of genes in accordance with their relative importance. (**E**) Accuracy and (**F**) error of 10-fold cross-validation in SVM-RFE algorithms, respectively. (**G**) The intersection of diagnostic biomarkers screened by three machine algorithms.

Diagnostic Efficacy of Diagnostic Biomarkers

Based on the expression of two genes, a diagnostic nomogram was constructed for RA to assess its diagnostic specificity and sensitivity (Figure 3A). ROC curves were generated to evaluate the diagnostic utility of individual genes and the nomogram. Figure 3B illustrated that VEGFB (0.819) and ARHGAP17 (0.978) had AUC values exceeding 0.75. In addition, the nomogram model (AUC = 0.981) based on two genes showed better diagnostic performance than two genes alone (Figure 3C). Based on the calibration curve analysis in Figure 3D, the nomogram model demonstrated comparable accuracy to the true positivity rate. The clinical decision curves revealed that the Nomogram model developed with two genes had a high predictive ability for RA, as the model curve outperformed the two threshold curves for benefits (Figure 3E).

Identification and Verification of Diagnostic Biomarkers

The diagnostic effectiveness of two genes for RA was validated on peripheral blood samples from three external datasets with RA. The AUC values of VEGFB and ARHGAP17 were 0.692 and 0.815 in GSE17755 (Figure 4A), respectively, and the diagnostic model showed promising efficacy in RA (AUC = 0.817) (Figure 4D). Besides, the AUC values of VEGFB and ARHGAP17 genes were 0.721 and 0.767 in GSE93272 (Figure 4B), respectively, and the diagnostic model showed good efficacy in RA (AUC = 0.794) (Figure 4E). The AUC values of VEGFB and ARHGAP17 genes were 0.922 and 0.945 in GSE205962 (Figure 4C), respectively, and the diagnostic model showed good efficacy in RA (AUC = 1.000) (Figure 4F).

In addition, the diagnostic biomarkers showed differential expression in the training and validation cohorts. The expression levels of ARHGAP17 and VEGFB in the peripheral blood of patients with RA were significantly decreased in GSE15573 (Figure 5A and B), GSE17755 (Figure 5C and D), GSE93272 (Figure 5E and F), and GSE205962 (Figure 5G and H) compared to healthy individuals. Besides, EA can increase the levels of VEGFB and ARHGAP17 in the peripheral blood of RA patients (Figure 6A and B), with comparable effectiveness to DMARDs such as IFX (Figure 6C and D), MTX (Figure 6E and F), and TCZ (Figure 6G and H).

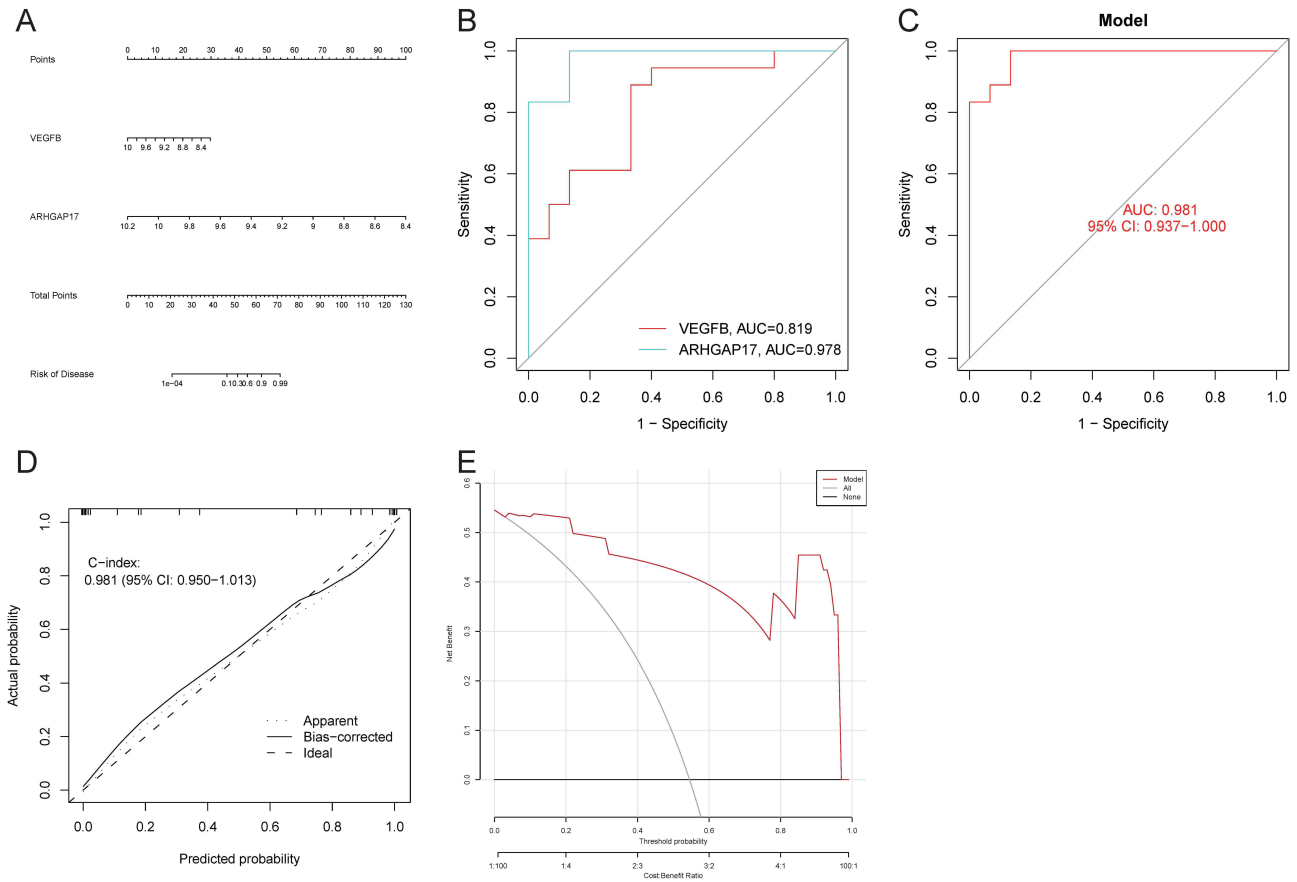

Figure 3 Construction of the nomogram model and efficacy assessment. (**A**) The nomogram of diagnostic biomarkers for risk prediction of RA. (**B**) The ROC curves of each diagnostic biomarker. (**C**) The ROC curve of the nomogram model. (**D**) The calibration curve of nomogram model prediction in RA. (**E**) DCA results to evaluate the clinical value of the nomogram model.

EA Demonstrated Analgesic Effects in CFA-Induced Mechanical Allodynia

Measurement of PWT in the ipsilateral hindpaws of rats showed hyperalgesia induced by CFA and antihyperalgesic effects of EA. As shown in Figure 7, the baseline values of PWT prior to injection of CFA did not exhibit significant differences across groups. Following the administration of CFA, the PWT of the CFA group and the CFA+EA group exhibited a significant decrease in comparison to the control group and the hyperalgesia endured for a minimum duration of one week. After receiving EA therapy, the rats in the CFA+EA group demonstrated a significant improvement in PWT starting from the first day as compared to the CFA group, indicating that EA significantly alleviated mechanical allodynia in CFA rats.

The qPCR analysis showed a significant reduction in ARHGAP17 and VEGFB mRNA expression levels in the peripheral blood of the CFA group compared to the control group. Conversely, EA can significantly increase the expression of ARHGAP17 and VEGFB in the peripheral blood of CFA rats (Figure 8A and B).

Discussion

This study identified 26 genes associated with the therapeutic effects of EA on RA. Machine learning algorithms were employed to identify two genes, ARHGAP17 and VEGFB, as potential diagnostic biomarkers, and their diagnostic efficacy was subsequently validated through the construction of a Nomogram model. Meanwhile, we demonstrated through various validation datasets that both diagnostic markers were significantly decreased in RA patients and exhibited excellent diagnostic performance. Furthermore, we found that these two biomarkers could effectively reflect the therapeutic effects of DMARDs and EA on RA, serving as prognostic indicators for evaluating treatment efficacy in RA. To further validate these findings, we established a CFA model, which revealed that the transcription levels of

https://doi.org/10.2147/JPR.S517733

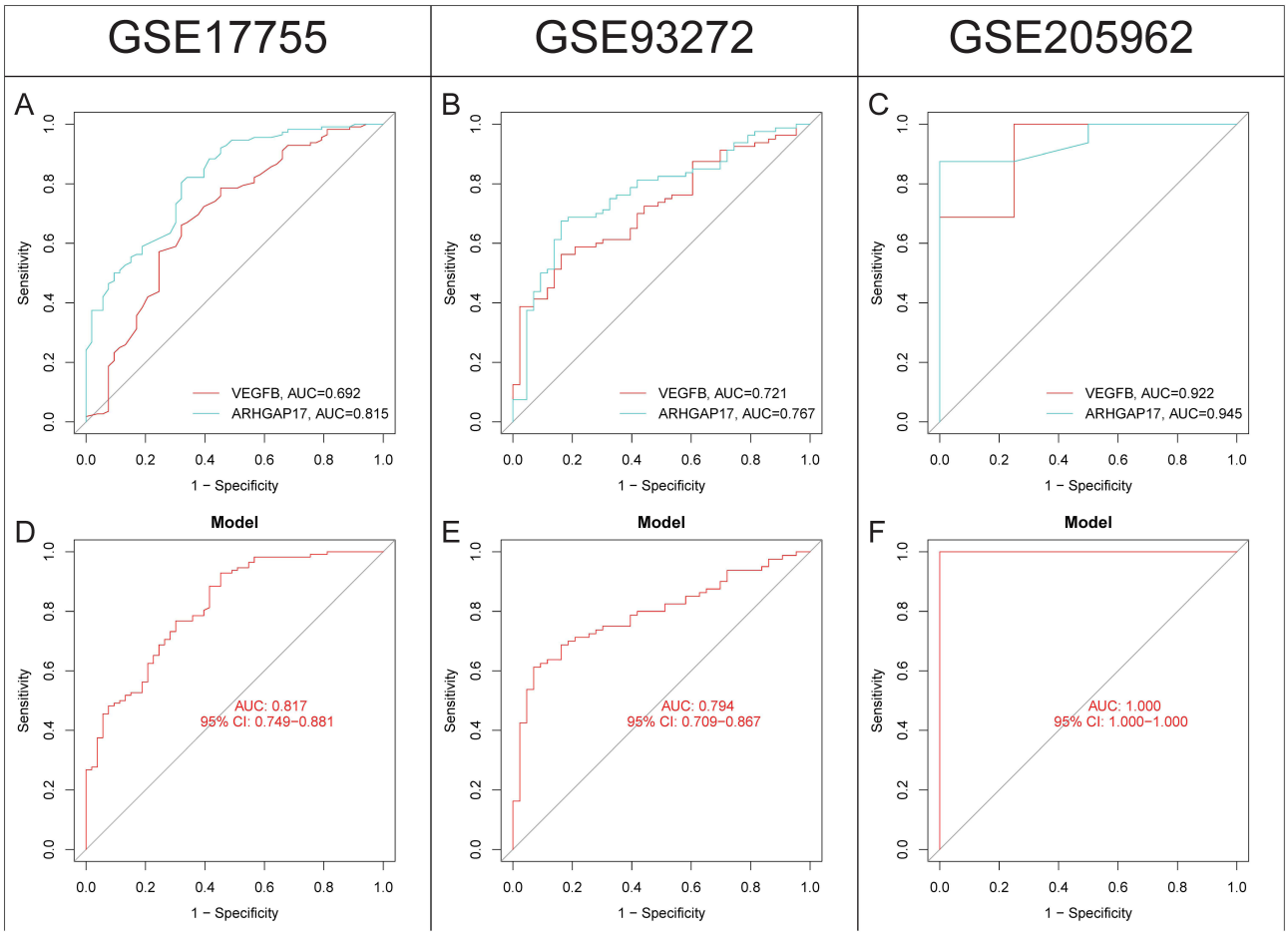

Figure 4 The ROC curves of each diagnostic biomarker and the nomogram model in GSE17755 (**A** and **D**), GSE93272 (**B** and **E**) and GSE205962 (**C** and **F**).

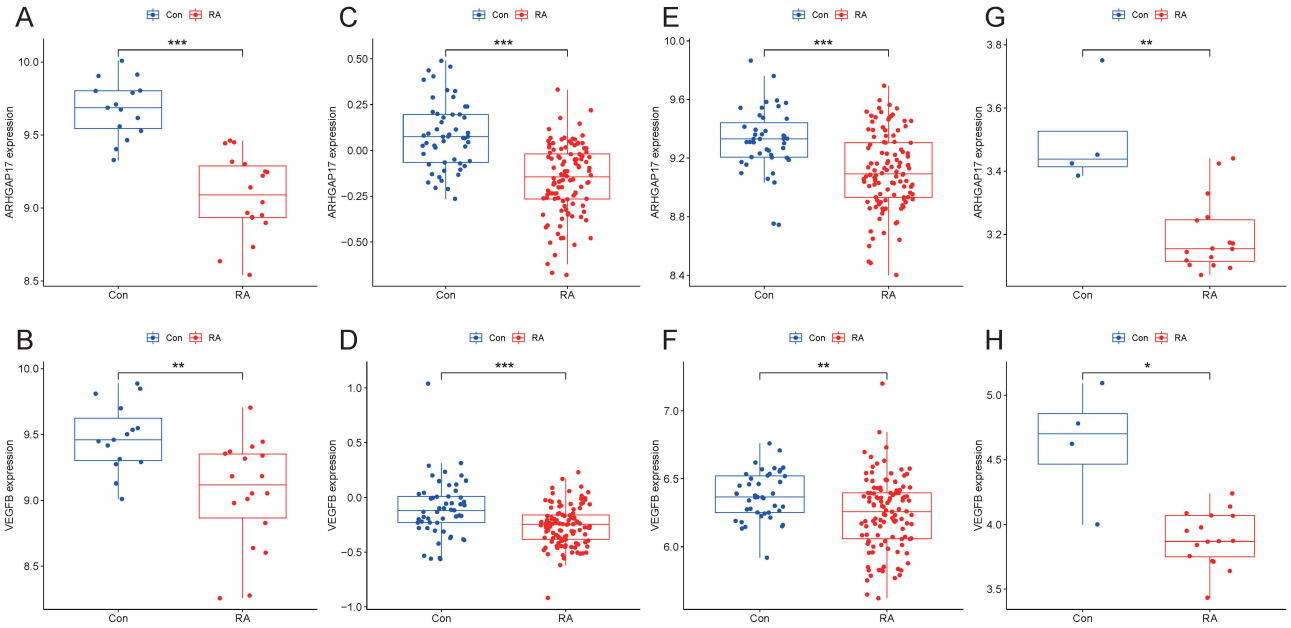

Figure 5 Expression levels of ARHGAP17 and VEGFB in the GSE15573 (**A** and **B**), GSE17755 (**C** and **D**), GSE93272 (**E** and **F**), and GSE205962 (**G** and **H**). *p < 0.05, **p < 0.01, ***p < 0.001, compared to the Control group.

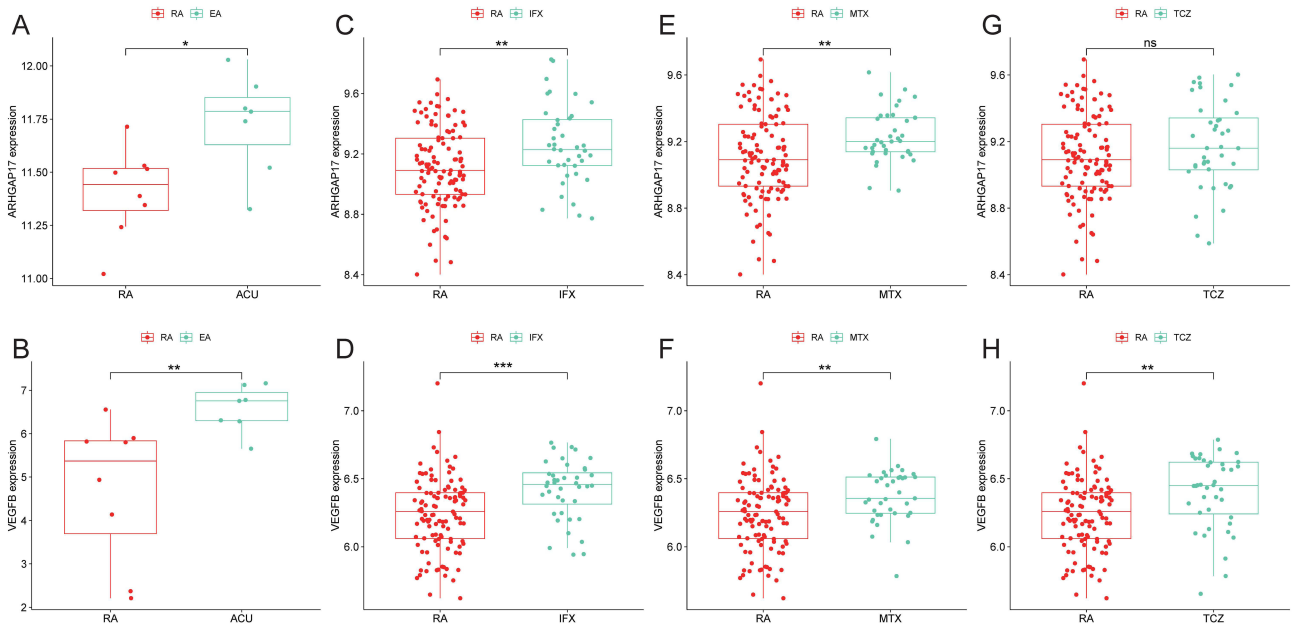

Figure 6 Comparison of ARHGAP17 and VEGFB expression levels following treatment with EA (**A** and **B**), IFX (**C** and **D**), MTX (**E** and **F**), and TCZ (**G** and **H**). *p < 0.05, **p < 0.01, ***p < 0.001, compared to the RA group.

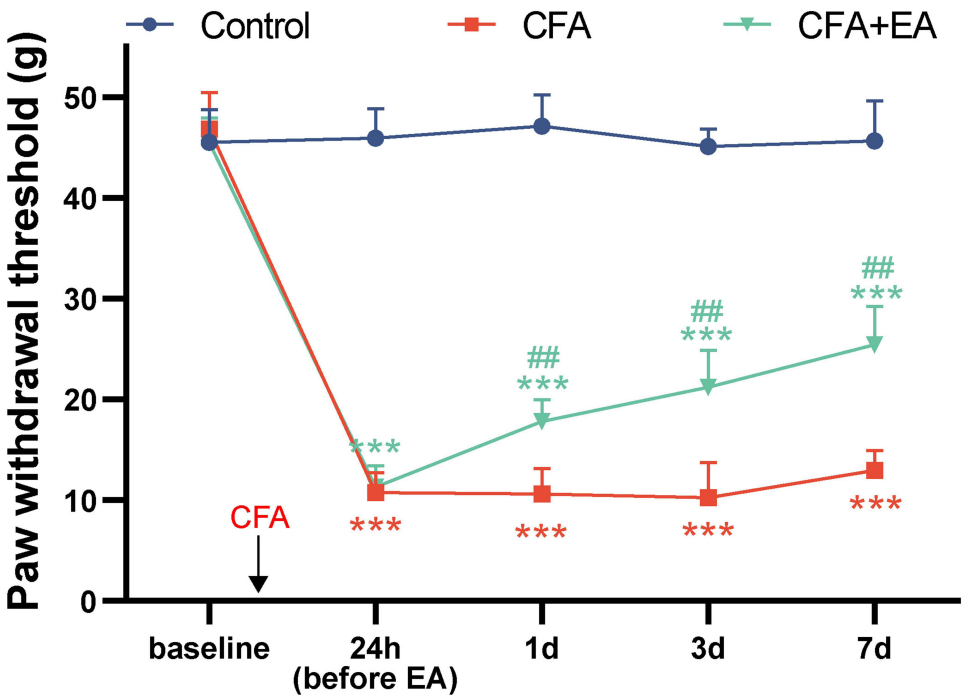

Figure 7 The effects of EA on mechanical allodynia induced by CFA. ***p < 0.001 compared to the control group; ##p < 0.01, compared to the CFA group.

ARHGAP17 and VEGFB were significantly reduced in the peripheral blood of CFA-treated rats. Notably, EA therapy reversed this reduction, suggesting its potential therapeutic benefits for RA.

Rho guanosine triphosphatases (GTPases) function as molecular switches and have been implicated in the dysregulation associated with the pathogenesis of RA.[21] The enzymatic activity of Rho GTPases is stringently regulated by Rho GTPase-activating proteins (GAPs), which play a crucial role in modulating signaling accuracy and preventing aberrant

https://doi.org/10.2147/JPR.S517733

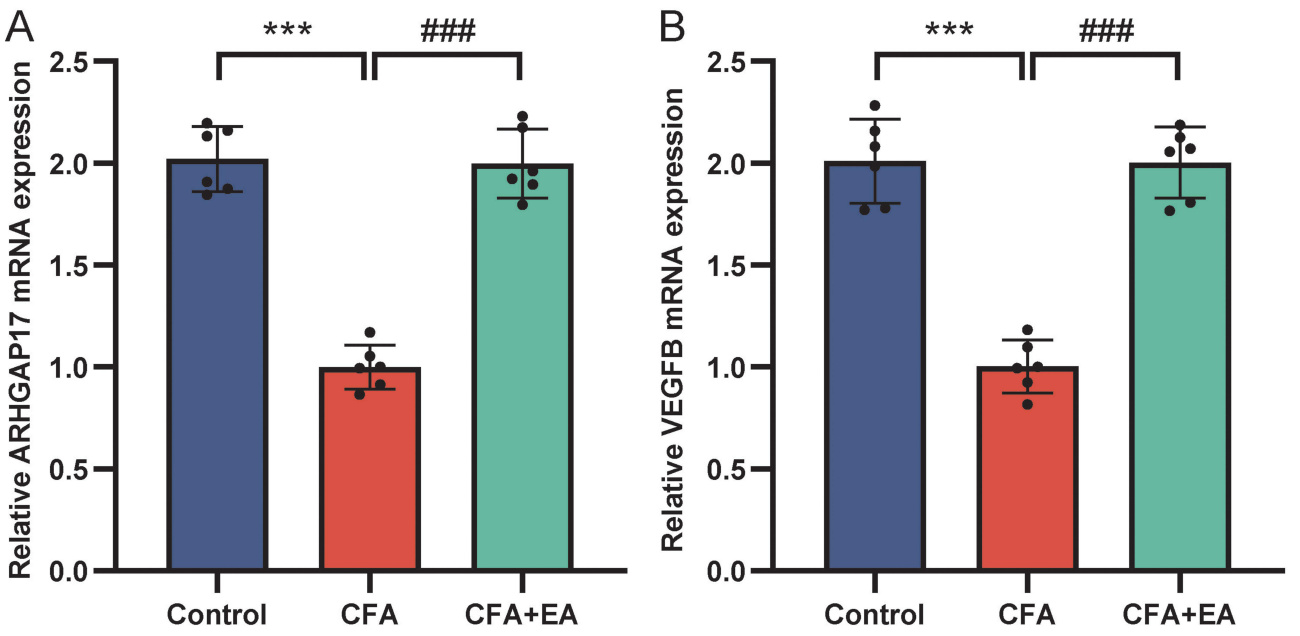

Figure 8 The effect of EA on regulating the diagnostic biomarkers. The mRNA expression of ARHGAP17 (**A**) and VEGFB (**B**) were analyzed by qPCR. ***p < 0.001 compared to the control group; ###p < 0.001 compared to the CFA group.

activation. ARHGAP17 (Rho GTPase Activating Protein 17), also known as RICH1, belongs to the GTPase-activating proteins (GAP) family, widely expressed in human tissues, and functions as a negative regulator of GTPases. Current research on ARHGAP17 has primarily focused on its role in cancer,[22] while the potential involvement of ARHGAP17 in the effects of EA remained unexplored. Notably, the Rho GTPase (RAC1) is involved in the progression of various pain conditions,[23–25] and EA has been shown to alleviate pain by suppressing RAC1 expression.[26] To date, no studies have established the diagnostic or therapeutic value of ARHGAP17 in RA. Interestingly, existing evidence indicated that ARHGAP17 may suppress RAC1 expression and reduce cellular apoptosis.[22] Our study demonstrated that EA can reverse the decreased expression of ARHGAP17 in the peripheral blood of CFA rats, suggesting that EA may exert its anti-inflammatory and analgesic effects by promoting ARHGAP17 expression, thereby inhibiting the activation of the Rho GTPase and mitigating the progression of RA.

Vascular endothelial growth factors (VEGFs) are the crucial molecule that promotes angiogenesis, which is a characteristic pathological feature of RA.[27] Notably, a previous study has demonstrated that serum VEGF levels in RA patients correlated positively with disease severity,[28] suggesting that VEGF may serve as a valuable molecular biomarker for evaluating the severity of RA. However, emerging evidence suggested that VEGF not only promoted inflammation and angiogenesis but also facilitated subchondral bone regeneration in arthritic joints.[29] A preliminary study found that promoting VEGF expression within the joint can enhance lymphatic drainage, thereby reducing the severity of RA.[30] As one of the subtypes of VEGF, VEGFB can be regulated by vagus nerve electrical stimulation, suppressing inflammatory responses through activation of the PI3K/AKT-FoxO3A-VEGF-A/B signaling cascade.[31] This study revealed that EA can upregulate VEGFB expression in the peripheral blood of RA patients and CFA rats. This finding appeared contradictory to previous research demonstrating that EA suppressed VEGF mRNA expression in synovial tissue of adjuvant arthritis rats.[32] We hypothesized that the inconsistent results may be due to differences in the regulation of VEGF subtypes by EA.

This study was not the first to apply bioinformatics analysis to identify potential biomarkers involved in EA treatment for RA. However, compared with previous research,[32] it incorporated a broader range of machine learning algorithms and validated the findings across multiple validation datasets. The present study has the following limitations: Firstly, the datasets employed in this study contained a relatively limited number of EA treatment cases. Additionally, we did not evaluate biomarker diagnostic efficacy across diverse demographic subgroups or perform batch-effect correction on the dataset. Secondly, due to experimental limitations, this study did not expand on the diagnostic efficacy of biomarkers in

clinical RA patients or the regulatory effects of EA on these biomarkers. Current animal models exhibited limited capacity to fully recapitulate the complex pathogenesis of RA, thereby constraining accurate assessment of diagnostic biomarker performance and EA therapeutic efficacy across disease subtypes. Therefore, further clinical experiments are needed to extend the application of biomarkers.

Conclusion

The present study identified two potential diagnostic biomarkers for RA using bioinformatics and machine learning approaches, and revealed that EA modulated the expression of these genes in peripheral blood. These findings not only provided new potential biomarkers for RA diagnosis but also offered novel therapeutic targets for EA-based treatment in RA management. However, further clinical trials are necessary to validate the diagnostic efficacy of biomarkers for different populations and the regulatory effects of EA on these biomarkers.

Abbreviations

CFA, Complete Freund's Adjuvant; DEGs, Differentially expressed genes; DMARDs, disease-modifying antirheumatic drugs; EA, Electroacupuncture; GEO, Gene Expression Omnibus; IFX, Infliximab; LASSO, Least absolute shrinkage and selection operator; MDG, Mean decrease Gini; MTX, Methotrexate; NSAIDs, Non-steroidal anti-inflammatory drugs; PWT, Paw withdrawal threshold; RA, Rheumatoid arthritis; ROC, Receiver operating characteristic; SVM-RFE, Support vector machine recursive feature elimination; TCM, Traditional Chinese Medicine; TCZ, Tocilizumab.

Data Sharing Statement

The datasets analyzed for this study can be found in the GEO (https://www.ncbi.nlm.nih.gov/geo/query/acc.cgi?acc = GSE15573, GSE59526, GSE17755, GSE205962, and GSE93272).

Funding

This research was fund by Shanghai Chinese Medicine Three-Year Action Plan Project (ZY(2021-2023)-0202, ZY(2021-2023)-0502).

Disclosure

The authors report no conflicts of interest in this work.

References

1. Xie Y, Fan KW, Guan SX, Hu Y, Gao Y, Zhou WJ. LECT2: a pleiotropic and promising hepatokine, from bench to bedside. *J Cell Mol Med*. 2022;26(13):3598–3607. doi:10.1111/jcmm.17407
2. Wan R, Fan Y, Zhao A, et al. Comparison of efficacy of acupuncture-related therapy in the treatment of rheumatoid arthritis: a network meta-analysis of randomized controlled trials. *Front Immunol*. 2022;13:829409. doi:10.3389/fimmu.2022.829409
3. Shang J, Xu J, Zhang Z, Tian L, He Y. The efficacy and safety of acupuncture-related therapy in the treatment of rheumatoid arthritis: a protocol for systematic review and network meta-analysis. *Medicine*. 2021;100(32):e26859. doi:10.1097/md.0000000000026859
4. Zhang Q, Tan Y, Wen X, Li F. Involvement of Neuropeptide Y within paraventricular nucleus in electroacupuncture inhibiting sympathetic activities in hypertensive rats. *Int J Hypertens*. 2022;2022:9990854. doi:10.1155/2022/9990854
5. Seca S, Kirch S, Cabrita AS, Greten HJ. Evaluation of the effect of acupuncture on hand pain, functional deficits and health-related quality of life in patients with rheumatoid arthritis--A study protocol for a multicenter, double-blind, randomized clinical trial. *J Integr Med*. 2016;14(3):219–227. doi:10.1016/s2095-4964(16)60254-6
6. Seca S, Patrício M, Kirch S, Franconi G, Cabrita AS, Greten HJ. Effectiveness of acupuncture on pain, functional disability, and quality of life in rheumatoid arthritis of the hand: results of a double-blind randomized clinical trial. *J Altern Complementary Med*. 2019;25(1):86–97. doi:10.1089/acm.2018.0297
7. Lee H, Lee JY, Kim YJ, et al. Acupuncture for symptom management of rheumatoid arthritis: a pilot study. *Clin Rheumatol*. 2008;27(5):641–645. doi:10.1007/s10067-007-0819-3
8. Ouyang BS, Gao J, Che JL, et al. Effect of electro-acupuncture on tumor necrosis factor-α and vascular endothelial growth factor in peripheral blood and joint synovia of patients with rheumatoid arthritis. *Chin J Integr Med*. 2011;17(7):505–509. doi:10.1007/s11655-011-0783-2
9. Zeng C, Bai X, Qin H, Wang H, Rong X, Yan J. Effect of adjuvant therapy with electroacupuncture on bone turnover markers and interleukin 17 in patients with rheumatoid arthritis. *J Tradit Chin Med*. 2019;39(4):582–586.
10. Zhang RB, Dong LC, Shen Y, et al. Electroacupuncture alleviates ulcerative colitis by targeting CXCL1: evidence from the transcriptome and validation. *Front Immunol*. 2023;14:1187574. doi:10.3389/fimmu.2023.1187574

11. Wie HS, Kim SN. Therapeutic components of acupuncture stimulation based on characteristics of sensory nerve and nervous signaling pathway. *J Integr Med*. 2025;23(2):106–112. doi:10.1016/j.joim.2025.02.002
12. Zhou S, Lu H, Xiong M. Identifying immune cell infiltration and effective diagnostic biomarkers in rheumatoid arthritis by bioinformatics analysis. *Front Immunol*. 2021;12:726747. doi:10.3389/fimmu.2021.726747
13. Cheng Q, Chen X, Wu H, Du Y. Three hematologic/immune system-specific expressed genes are considered as the potential biomarkers for the diagnosis of early rheumatoid arthritis through bioinformatics analysis. *J Transl Med*. 2021;19(1):18. doi:10.1186/s12967-020-02689-y
14. Li L, Zhou D, Liu Q, et al. Network analysis indicating the pharmacological mechanism of Yunpi-Qufeng-Chushi-prescription in prophylactic treatment of rheumatoid arthritis. *BMC Complement Med Therap*. 2021;21(1):142. doi:10.1186/s12906-021-03311-4
15. Hui P, Zhou S, Cao C, Zhao W, Zeng L, Rong X. The elucidation of the anti-inflammatory mechanism of EMO in rheumatoid arthritis through an integrative approach combining bioinformatics and experimental verification. *Front Pharmacol*. 2023;14:1195567. doi:10.3389/fphar.2023.1195567
16. Khadour FA, Khadour YA, Xu T. Electroacupuncture delays the progression of juvenile collagen-induced arthritis via regulation NLRP3/ NF-κB signaling pathway -mediated pyroptosis and its influence on autophagy. *Clin Rheumatol*. 2025;44(4):1713–1728. doi:10.1007/s10067-025-07354-7
17. Dong SY, Zhou Y, Wang XC, Du ZH, Ye TS. Electroacupuncture attenuates bone erosion and promotes macrophage polarization in a mouse model of collagen-induced arthritis. *Acupunct Med*. 2025;9645284251331991. doi:10.1177/09645284251331991
18. Ellis K, Kerr J, Godbole S, Lanckriet G, Wing D, Marshall S. A random forest classifier for the prediction of energy expenditure and type of physical activity from wrist and Hip accelerometers. *Physiol Meas*. 2014;35(11):2191–2203. doi:10.1088/0967-3334/35/11/2191
19. Alolga RN, Opoku-Damoah Y, Alagpulinsa DA, et al. Metabolomic and transcriptomic analyses of the anti-rheumatoid arthritis potential of xylopic acid in a bioinspired lipoprotein nanoformulation. *Biomaterials*. 2021;268:120482. doi:10.1016/j.biomaterials.2020.120482
20. Vivancos GG, Verri WA, Cunha TM, et al. An electronic pressure-meter nociception paw test for rats. *Braz J Med Biol Res*. 2004;37(3):391–399. doi:10.1590/s0100-879x2004000300017
21. Zeng R, Zhuo Z, Luo Y, Sha W, Chen H. Rho GTPase signaling in rheumatic diseases. *iScience*. 2022;25(1):103620. doi:10.1016/j.isci.2021.103620
22. Wang L, Yang X, Wan L, Wang S, Pan J, Liu Y. ARHGAP17 inhibits pathological cyclic strain-induced apoptosis in human periodontal ligament fibroblasts via Rac1/Cdc42. *Clin Exp Pharmacol Physiol*. 2020;47(9):1591–1599. doi:10.1111/1440-1681.13336
23. Wan Y, Zhou J, Zhang P, Lin X, Li H. Inhibition of spinal Rac1 attenuates chronic inflammatory pain by regulating the activation of astrocytes. *Cell Signalling*. 2024;114:110972. doi:10.1016/j.cellsig.2023.110972
24. Chen Z, Zhang S, Nie B, et al. Distinct roles of srGAP3-Rac1 in the initiation and maintenance phases of neuropathic pain induced by paclitaxel. *J Physiol*. 2020;598(12):2415–2430. doi:10.1113/jp279525
25. Xu L, Yang L, Wu Y, et al. Rac1/PAK1 signaling contributes to bone cancer pain by regulation dendritic spine remodeling in rats. *Mol Pain*. 2023;19:17448069231161031. doi:10.1177/17448069231161031
26. Wu Q, Cai C, Ying X, et al. Electroacupuncture inhibits dendritic spine remodeling through the srGAP3-Rac1 signaling pathway in rats with SNL. *Bio Res*. 2023;56(1):26. doi:10.1186/s40659-023-00439-0
27. MacDonald IJ, Liu SC, Su CM, Wang YH, Tsai CH, Tang CH. Implications of angiogenesis involvement in arthritis. *Int J Mol Sci*. 2018;19(7):2012. doi:10.3390/ijms19072012
28. Kim JW, Kong JS, Lee S, et al. Angiogenic cytokines can reflect the synovitis severity and treatment response to biologics in rheumatoid arthritis. *Exp Mol Med*. 2020;52(5):843–853. doi:10.1038/s12276-020-0443-8
29. Rong M, Liu D, Xu X, et al. A superparamagnetic composite hydrogel scaffold as in vivo dynamic monitorable theranostic platform for osteoarthritis regeneration. *Adv Mater*. 2024;36(35):e2405641. doi:10.1002/adma.202405641
30. Luo B, Wu Y, Liu SL, et al. Vagus nerve stimulation optimized cardiomyocyte phenotype, sarcomere organization and energy metabolism in infarcted heart through FoxO3A-VEGF signaling. *Cell Death Dis*. 2020;11(11):971. doi:10.1038/s41419-020-03142-0
31. Zhu J, Su C, Chen Y, Hao X, Jiang J. Electroacupuncture on ST36 and GB39 acupoints inhibits synovial angiogenesis via downregulating HIF-1α/VEGF expression in a rat model of adjuvant arthritis. *Evid Based Complement Alternat Med*. 2019;2019:5741931. doi:10.1155/2019/5741931
32. Shen C, Gu B, Tang M, et al. Biomarkers identification of early rheumatoid arthritis via bioinformatics approach and experimental verification. *Ann Clin Lab Sci*. 2024;54(5):661–670.